THE PUBLISHING HOUSE
OF THE ROMANIAN ACADEMY

PROCEEDINGS OF THE ROMANIAN ACADEMY, Series A,
Volume 19, Number 1/2018, pp. 29–34

ELECTRICALLY ACTIVE TRAPPING STATES SLOWING RECOMBINATION IN THALLIUM BROMIDE CRYSTALS AT LOW TEMPERATURES

Vaidotas KAŽUKAUSKAS, Rokas GARBAČAUSKAS, Slavomir SAVICKI

Vilnius University, Semiconductor Physics Department and Institute of Applied Research,
Saulėtekio al. 3, Room A324, LT-10257 Vilnius, Lithuania

Corresponding author: Vaidotas KAŽUKAUSKAS, E-mail: vaidotas.kazukauskas@ff.vu.lt

Abstract. The frozen enhanced photoconductivity effects were observed in thallium bromide (TlBr) crystals below 200 K after the band-to-band light excitation. This state could be thermally quenched above 180 K, because of the emptying of the trapping states having activation energy of 0.63–0.65 eV. The strong superlinear dependence of the persistent conductivity on the applied electric field strength was evidenced too. These phenomena could be due to the filling of the trapping states with the thermal activation energies of 0.08–0.12 eV. The electrically active trap level at 0.35 eV was identified by the thermally stimulated currents; moreover several photoactive defects with optical activation energies of 0.55, 0.83, 1.1, 1.32, and 1.65 eV were revealed.

Key words: TlBr, trapping states, enhanced (photo-) conductivity, thermal quenching.

1. INTRODUCTION

Thallium bromide (TlBr) is characterized by several electro-physical parameters that make it extraordinarily suitable for applications as the room temperature radiation detector in X-ray and γ-ray spectroscopy. This semiconducting material has the wide energy bandgap –2.68 eV, high density –7.56 g/cm^3 and high atomic numbers – Tl: 81 and Br: 35 [1–3]. The wide bandgap assures the low thermal charge carrier generation rate, thus the material has high resistivity, exceeding 10^{10} Ohm-cm at room temperature, low dark current and device noise. The high density and atomic numbers ensure a high photon stopping efficiency. The pixelated TlBr γ-rays detectors have demonstrated energy resolutions of 6.7 keV (5.5%) FWHM and 22.3 keV (3.4%) FWHM for 122 and 662 keV gamma-rays, respectively [2, 3]. The electron $\mu\tau$ product, which is important for the device sensitivity, is up to 4.1×10^{-3} cm^2/V at room temperature [4]. Nevertheless, as it was demonstrated recently, TlBr detector properties and electrical parameters depend sensitively on the peculiarities of technological processes, resulting in varied defect densities [5].

Moreover, one of the main problems that still essentially limits the practical applicability of TlBr is the ionic conductivity phenomenon, which strongly depends on the temperature [6] and causes instability of device characteristics [7]. This results in, e.g., degradation of spectroscopic performance because of the polarization phenomena if devices are operated at the room temperature [2]. So, electro-migration of impurities in TlBr was reported in [8]. Furthermore, ionic transport and resulting defect reactions might cause appearance of the Schottky defects [9]. Formation of Tl and Br vacancy pair in the bulk is accomplished by creation of new Tl and Br occupied sites on the crystal surface. In addition to the surface, grain boundaries and dislocations can also serve as sources and/or sinks for defect formation and annihilation [9]. The enthalpies of Schottky defect formation (0.91 eV), that of cation migration (0.51 eV), and anion migration (0.28 eV) were evaluated in [10].

Apart from that, charge carrier transport and (photo-) electrically active defect properties of TlBr are still relatively little investigated, depending on the excitation conditions.

In TlBr, as in all high resistivity semiconducting materials, carrier generation and transport phenomena vary significantly with temperature and upon light excitation, enabling to reveal effects related to defect

levels and inhomogeneities of the crystals [11–13]. Therefore, it was our task to investigate (photo-) conductivity properties of TlBr in the temperature region from the room temperature down to the liquid nitrogen temperature. As at temperatures below 240 K ionic conductivity of TlBr is negligible [13], such situation is beneficial for the analysis of charge transport.

2. SAMPLES AND EXPERIMENT

TlBr single crystals were grown by the Bridgman–Stockbarger method. They were cut, mechanically and chemically polished to produce the samples with dimensions of about 4×2×1 mm^3. The gold electrodes were evaporated on the ends of the samples. We have investigated photoconductivity spectra, thermally stimulated currents (TSCs) and current transients in the temperature range from 300 K down to about 100 K, depending on the applied bias voltage. The bias was supplied from Keithley 6430B Source Measure Unit; the same device measured current flowing through the sample.

To investigate the spectral dependencies of photocurrent samples were excited by the monochromatic light from the Leitz monochromator. To discriminate the defect levels the spectra were analysed using Lucovsky photoionization model [14]:

$$I \sim n_M \Delta E_M^{0.5} \left(h\nu - \Delta E_M\right)^{1.5} / \left(h\nu\right)^3, \tag{1}$$

where ΔE_M is the optical activation energy of the deep trap, n_M is density of the trapped carriers, and $h\nu$ is quantum energy of the exciting light.

Carrier transport and trapping were investigated by the Thermally Stimulated Current (TSC) spectroscopy as described in detail in [15]. The samples were cooled down in the Liquid Nitrogen cryostat in the dark and the spectral dependencies of their photoconductivity were scanned to assure selective excitation of the optically active defect states. After the light was turned off, the long lasting current relaxation kinetics were measured to assure sample relaxation. After that, the samples were heated at a 10 K/min rate to measure TSCs. To evaluate possible effects caused by several closely located trapping centers, the informative multiple heating technique was used, that enables sequential emptying of the levels, assuring in that way their discrimination [15].

The dark currents at the same bias were measured too. They were subtracted from the TSC data obtained after the light excitation.

The TSCs caused by the thermal carrier generation from the traps can be described as [16]:

$$I = \frac{1}{2} eLAf_t n_{t0} \exp\left[-\frac{E_t}{kT} - \frac{f_t kT^2}{\beta(E_t + kT)} \exp\left(-\frac{E_t}{kT}\right)\right], \tag{2}$$

where n_{t0} is the carrier density at the traps having activation energy E_t, T is the temperature, β is the heating rate, k is the Boltzmann constant, f_t is the carrier attempt-to-escape frequency, e is the elementary charge, L is the layer thickness, and A is the sample area.

The initial filling of the traps n_{t0} was evaluated by integrating experimental curves over time. The obtained values have demonstrated good coincidence with the fitting parameters.

3. RESULTS AND DISCUSSION

Usually in TlBr the photoconductivity is low at 300 K as compared with the dark conductivity, therefore any defect-related features could not be identified by photospectroscopy at this temperature [17]. The dark current decreases exponentially with decreasing temperature, the thermal activation energy of this process being ~ (0.78–0.8 eV) [13]. Therefore, at low temperatures the effect of photoconductivity increases notably, enabling identification of defect levels, depending on the sample prehistory, i.e., its excitation by light and/or voltage [13]. In Fig. 1 experimental spectral dependencies at 240 K and their fitting by Eq. (1) are presented. A maximum caused by the band-to-band carrier generation is evident at about 2.75 eV. Current drop at the high-energy side of this maximum is associated with the increasing absorption and

intensifying surface recombination. The following photoionization energies were evaluated by fitting the experimental curves: 0.55, 0.83, 1.1, 1.32, and 1.65 eV. The recharge of the trap with the activation energy of 1.65 eV could induce carrier mobility variations, observed and reported in Ref. [13]. Characteristically defect bands in the region between 1 eV and 2.5 eV were dependent on sample pre-excitation. The defect-related shoulders at about 0.83 and 1.1 eV used to appear if the spectra were scanned from the high to the low quantum energies. Meanwhile influence of the levels at 1.32 and 1.65 eV used to decrease if the sample was kept biased for several hours [13].

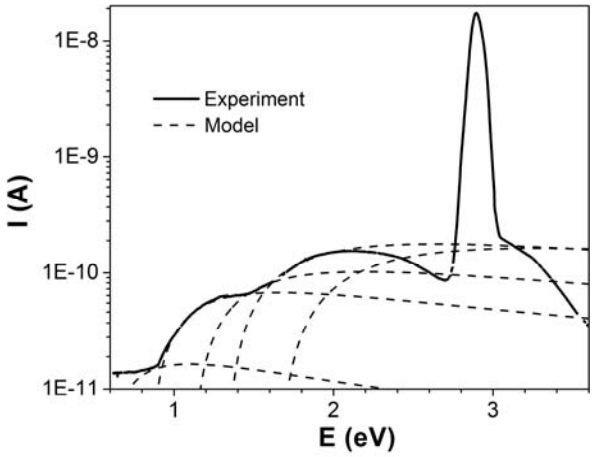

Fig. 1 – Photocurrent spectra (solid line) and its fitting (dashed curves) at 240 K.

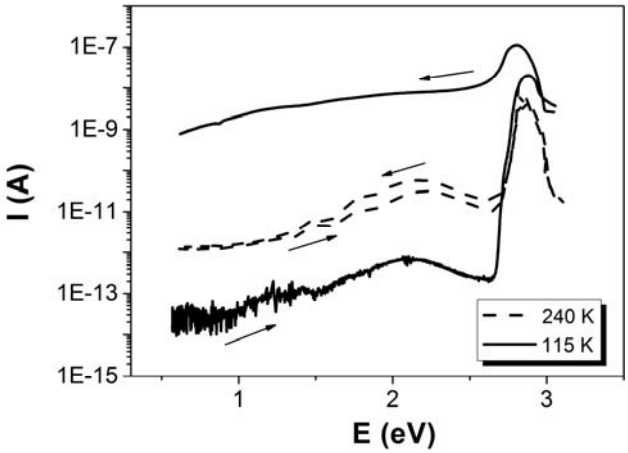

Fig. 2 – Photocurrent spectra at different temperatures. First, quantum energy was increased; afterwards it was decreased as indicated by the arrows.

Similar complicated defect structure was also revealed by PL [18, 19]. In [18] the PL between 1.5–2.0 eV was observed under X-ray excitation. It was ascribed to the diffusion-controlled recombination. Meanwhile in [19] PL at 1.1 eV was observed in the short-lived absorption spectra under pulsed electron beam excitation, and it was explained to be due to the hole trapped at cation vacancy ($Tl^{2+}V^{c-}$). This center can be created if holes become trapped on the pre-irradiation vacancy, as well as result from the radiation-induced Frenkel pair formation ($Tl^{2+}V^{c-}$ and interstitial thallium atom Tl_i^0). Our results imply that such vacancy can also appear due to the illumination by light, even if the intensity of light, from the monochromator, is low. The more detailed analysis of the results obtained at 240 K is presented in [13].

In Fig. 2 spectral dependencies of photoconductivity of the same sample is presented at different temperatures: 240 K and 115 K. In order to prevent sample pre-excitation by the high energy quanta, the spectral scans were started from the low quantum energy. Afterwards the scans were performed in an opposite direction. By increasing the quantum energy, the spectra measured at both temperatures coincide in detail, thought the dark current is considerably lower at low temperature.

Notably, it is seen in Fig. 2 that the spectra scanned in both directions at 240 K (and down to about 190 K) nearly coincide, indicating, that no long-lasting effects take place. In contrast, at lower temperatures (below 180 K) after the excitation of the sample by the intrinsic light, its photosensitivity remains by about four orders of magnitude higher than before the excitation. Moreover, the characteristic defect shoulders are no longer seen. This is caused by the appearance of the slow relaxation of the photocurrent called persistent photoconductivity (PPC) [20], see Fig. 3. The long lasting current and carrier mobility relaxations that could be attributed to this phenomenon were observed also in other high resistivity semiconductors, as, e.g., semiinsulating GaAs [21–23]

Another peculiar feature observed in samples pre-excited by the above-band-gap light is a strong superlinear dependence of the current on applied electric field. In Fig. 4 it is seen that upon increasing quantum energy, the photocurrent depends linearly on the applied electric field, meanwhile during the back scan differences in the photocurrent are up to several orders of magnitude.

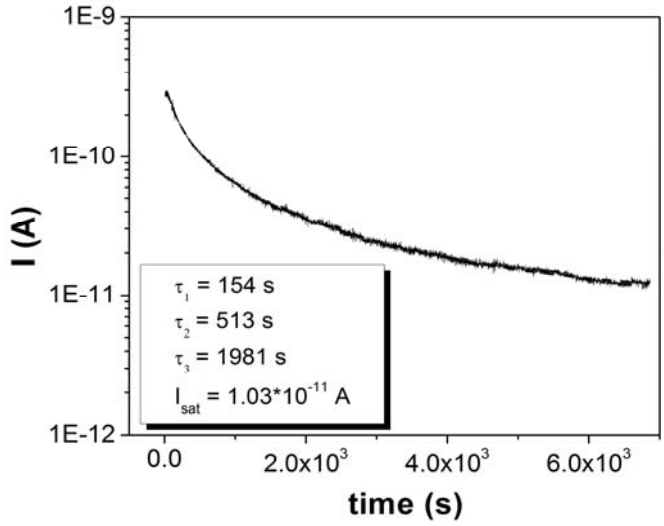

Fig. 3 – Current decay after the pre-excitation by the above-band-gap light.

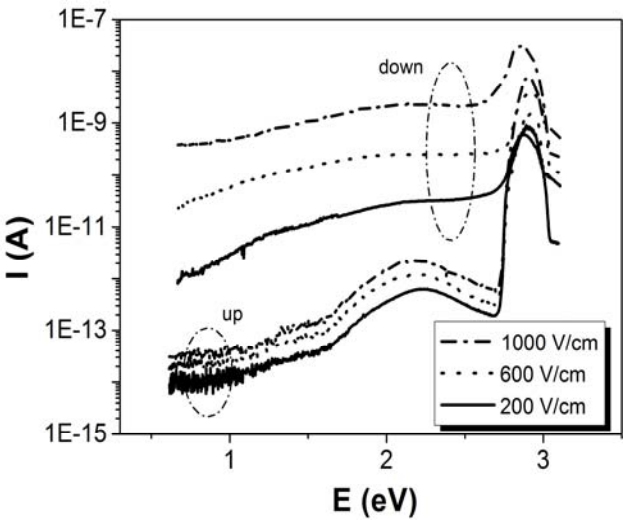

Fig. 4 – Photocurrent spectra at 115 K measured at different fields. First, quantum energy was increased; afterwards it was decreased.

In Fig. 3 the long-lasting current relaxation kinetics after the excitation of the sample by the intrinsic light is presented. The dotted line indicates fitting of the experimental decay curve by a sum of three exponents with different time constants as indicated on figure. Characteristically, the current does not relax to zero, but is saturating at the constant value level I_{sat} instead. The effect of persistent photoconductivity is related with the inability of the light generated to recombine, because they become trapped in trapping states. Such trapping states could be related with potential inhomogeneities of the band gap edges. Therefore, carriers become separated in space, and prior to recombination they have to gain additional energy to escape from the traps and to move in space [20]. In Ref. [20] it is stated, however, that the current usually relaxes following the single exponential dependence. In contrast, in our case a sum of three exponents was necessary to fit the experimental dependence, indicating a quite complex effect. Even the single stretched exponent was not enough for the fitting:

$$I_{SC} = I_{SC}(t=0)\exp\left[\left(-\frac{t}{\tau}\right)^{\beta}\right], \tag{3}$$

$$t_{1/2} = \tau(\ln 2)^{1/\beta}. \tag{4}$$

Here τ and β are characteristic parameters of the stretched exponent, and $t_{1/2}$ is the half-lifetime of the relaxation.

To investigate these trapping states with the low recombination probability at low temperatures we have analyzed the thermally stimulated currents. In Fig. 5 the experimental TSC measured at 200 V/cm electric field is indicated by the dotted line. Appearance of two current peaks with different activation energies is seen at lower temperatures. Meanwhile close to the room temperature TSC curves is coinciding with the dark current having activation energy of about 0.65 eV. Upon increasing electric field strength the strong nonlinear dependence of the current is clearly seen up to the temperatures of about 180–200 K. At higher temperatures the linear dependence of the current of the applied electric field becomes prevailing again.

To analyze such behavior in more detail, TSCs in repetitive heating mode were measured as presented in Fig. 6. At lower temperatures a wide and high TSC peak appears in all three curves, having thermal activation energy values of about 0.065–0.08 eV. In the following heating cycles these values increase up to 0.11–0.12 eV. This could be explained by the fact that if carriers are thermally generated from the potential wells of the band gap edges, in each temperature scan the effective depth of the partially emptied wells is increasing.

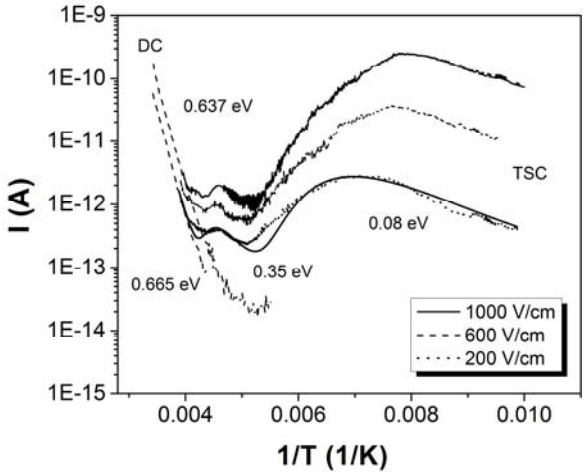

Fig. 5 – TSCs measured at different fields. The dark currents measured without light excitation are shown by dashed curves. At 200 V/cm TSC is presented by the dotted line and its fitting is shown by the solid line.

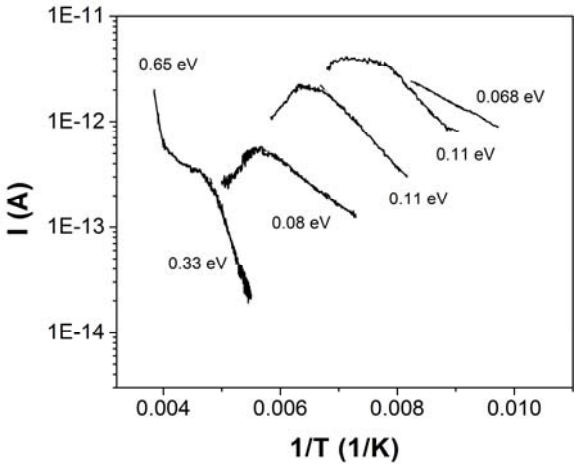

Fig. 6 – TSCs obtained by repetitive heating. The numbers indicate thermal activation energies.

After these shallowest traps become emptied, carrier generation from deeper traps with the thermal activation energy of about 0.33 eV begins. The emptying of this level occurs at about 220 K, as it is indicated by the flattening of the TSC curve. After that, the thermal generation with the activation energy of 0.65 eV starts, which is close to the values of 0.68–0.7 eV in Refs. [17, 24]. We have used these experimental values as model parameters to fit the TSC curve in Fig. 5 by using Eq. (2).

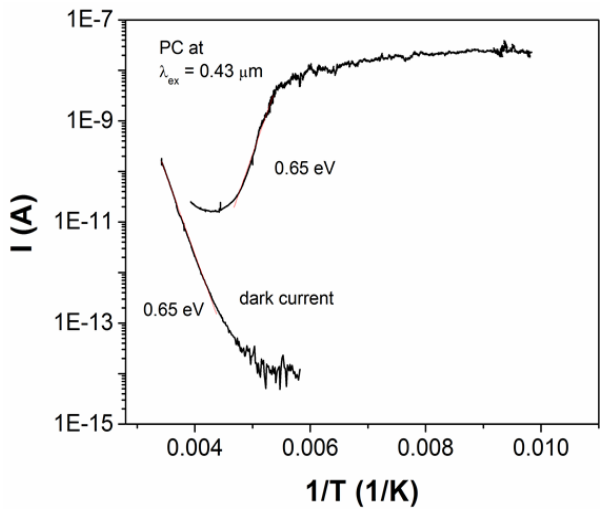

Fig. 7 – Temperature dependencies of the dark- and photo-currents measured from lowest temperatures upon the above-band-gap light excitation.

The presence of the defect states, which, depending on their filling might start acting as recombination centers, is proved by the thermal quenching effect in the illuminated samples.

In Fig. 7 the temperature dependencies of the dark current and photocurrent upon band-to-band light excitation are shown. They were measured starting from the lowest temperatures. The photocurrent exceeds much the TSCs, and it remains nearly stable up to ~180 K. At higher temperatures, the current starts decreasing with ~ 0.64 eV activation energy. Such thermal quenching of photoconductivity is well known, in particular in A_2B_6 semiconductors [25]. It is caused by the thermal emptying of the recombination centers, which, when filled, cannot trap carriers. Notably, activation energies of both dark current and thermal quenching are similar. This is a proof that thermal quenching could be caused by the emptying of the trap at about 0.65 eV.

4. SUMMARY AND CONCLUSIONS

We have identified persistent conductivity effects in TlBr at the temperatures below 200 K and down to 100 K. The conductivity values in this state have demonstrated the strong superlinear dependence on the applied electric field strength. The long lasting photoconductivity decays were initiated by intrinsic light excitation of the samples. The observed phenomena were associated with the filling of the trapping states having thermal activation energy of about 0.08–0.12 eV. The enhanced photoconductivity could be thermally quenched above 180 K. The quenching is presumably initiated by the emptying of the trapping states with activation energy of about 0.63–0.65 eV.

REFERENCES

1. P.J. SELLIN, *Recent advances in compound semiconductor radiation detectors*, Nucl. Instrum. Meth. A, **513**, pp. 332–339, 2003.
2. K. HITOMI, M. MATSUMOTO, O. MUROI, T. SHOJI, Y. HIRARATE, *Thallium bromide optical and radiation detectors for X-ray and gamma-ray spectroscopy*, IEEE Trans. Nucl. Sci., **49**, pp. 2526–2529, 2002.
3. K. HITOMI, M. MATSUMOTO, O. MUROI, T. SHOJI, Y. HIRARATE, *Characterization of thallium bromide crystals for radiation detector applications*, J. Cryst. Growth, **225**, pp. 129–133, 2001.
4. K. HITOMI, T. ONODERA, T. SHOJI, Y. HIRATATE, Z. HE, *TlBr gamma-ray spectrometers using the depth sensitive single polarity charge sensing technique*, IEEE Transactions on Nuclear Science, **55**, pp.1781–1784, 2008.
5. R.A. DOS SANTOS, C.H. DE MESQUITA, J.B.R. DA SILVA, C. DE MELO FERRAZ, F.E. DA COSTA, J.F.T. MARTINS, R.F. GENNARI, M.M. HAMADA, *Influence of impurities on the radiation response of the TlBr semiconductor crystal*, Advances in Materials Science and Engineering, 1750517, 2017.
6. T. ONODERA, K. HITOMI, T. SHOJI, *Spectroscopic performance and long-term stability of thallium bromide radiation detectors*, Nucl. Instrum. Meth. A, **568**, pp. 433–436, 2006.
7. K. HITOMI, T. SHOJI, K. ISHII, *Advances in TlBr detector development*, J. Cryst. Growth, **379**, pp. 93–98, 2013.
8. K.H. KIM, E. KIM, H. KIM, R. TAPPERO, A.E. BOLOTNIKOV, G.S. CAMARDA, A. HOSSAIN, L. CIRIGNANO and R.B. JAMES, *Electro-migration of impurities in TlBr*, J. Appl. Phys., **114**, 133701 ,2013.
9. S.R. BISHOP, H.L. TULLER, M. KUHN, G. CIAMPI, W. HIGGINS, K.S. SHAH, *Kinetics of Schottky defect formation and annihilation in single crystal TlBr*, Phys. Chem. Chem. Phys., **15**, pp. 11926–11930, 2013.
10. S.R. BISHOP, W. HIGGINS, G. CIAMPI, A. CHURILOV, K.S. SHAH, H.L. TULLER, *The defect and transport properties of donor doped single crystal TlBr*, J. Electrochem. Soc., **158**, pp. J47–J51, 2011.
11. J. VAITKUS, V. KAŽUKAUSKAS, R. KILIULIS, J. STORASTA, *Recognition of point defects and clusters and their distribution in semiinsulating GaAs*, Inst. Phys. Conf. Ser., **136**, pp. 755–760, 1994.
12. R. KILIULIS, V. KAŽUKAUSKAS, J. STORASTA, J.-V. VAITKUS, *Charge redistribution and potential barrier reconstruction in SI GaAs caused by EL2 state change*, J. de Physique I, **6**, pp. 1165–1187, 1996.
13. V. KAŽUKAUSKAS, A. ZIMINSKIJ, J.V. VAITKUS, V. GOSTILO, M. SHOROHOV, *Photoelectrical properties of TlBr related to ionic transport and presence of defects,* Nucl. Instrum. Meth. A, **607**, pp. 123–125, 2009.
14. G. LUCOVSKY. *On the photoionization of deep impurity centers in semiconductors,*Solid State Comm., **3**, pp. 299–302, 1965.
15. G. KAVALIAUSKIENĖ, V. KAŽUKAUSKAS, V. RINKEVIČIUS, J. STORASTA, J.V. VAITKUS, R. BATES, V. O'SHEA, K.M. SMITH, *Thermally stimulated currents in semi-insulating GaAs Schottky diodes and their simulation*, Appl. Phys. A – Mater. Sci. Proc., **69**, pp. 415–420, 1999.
16. J.G. SIMMONS, G.W. TAYLOR, *High-field isothermal currents and thermally stimulated currents in insulators having discrete trapping levels*, Phys. Rev. B, **5**, pp. 1619–1629, 1972.
17. V. KAŽUKAUSKAS, A. JURGILAITIS, J.-V. VAITKUS, *Analysis of photoelectrical and current transient behavior in TlBr*, Proc. SPIE, **6596**, C5960, 2007.
18. L. GRIGORJEVA, D. MILLERS, *The model of recombination process TlBr*, Nucl. Instrum. Meth. B, **191**, pp. 131–134, 2002.
19. L. GRIGORJEVA, D. MILLERS, *Excitonic processes in thallous halides excited by electron beam*, Electrochem. Soc. Proc., **98**, pp. 438–443, 1998.
20. M.K. SHEINKMAN, A.Y. SHIK, *Long-term relaxation and residual conductivity of semiconductors (review)*, Sov. Phys. Semicond., **10**, pp. 128–142, 1976.
21. V. KAŽUKAUSKAS, *Influence of defect inhomogeneities on the Hall mobility and concentration in undoped GaAs*, J. Appl. Phys., **84**, pp. 2053–2061, 1998.
22. V. KAŽUKAUSKAS, J. VAITKUS, *Investigation of transient transport and recombination phenomena in semiinsulating GaAs, Z. Phys. B-Condensed Matter*, **94**, pp. 401–407, 1994.
23. J. VAITKUS, R. BAUBINAS, E. GAUBAS, K. JARAŠIŪNAS, R. JAŠINSKAITE, V. KAŽUKAUSKAS, E. KUPRUSEVIČIUS, J. MATUKAS, V. PALENSKIS, J. STORASTA, M. SŪDŽIUS, R. TOMAŠIŪNAS, *GaAs peculiarities related with inhomogeneities and the methods for reveal of their properties,* Nucl. Instrum. Meth. A, **466**, pp. 39–46, 2001.
24. J. VAITKUS, J. BANYS, V. GOSTILO, S. ZATOLOKA, A. MEKYS, J. STORASTA, A. ŽINDULIS, *Influence of electronic and ionic processes on electrical properties of TlBr crystals,* Nucl. Instrum. Meth. A, **546**, pp. 188–191, 2005.
25. R.H. BUBE, *Photoconductivity of Solids*, John Wiley and Sons, Inc., New York, 1960.

Received May 12, 2017